IN VIVO AND IN VITRO EFFECTS OF BIOSYNTHESIZED ZnNPs AND AgNPs USING SESAMUM INDICUM SEEDS AGAINST MDR ENTEROCOCCUS HIRAE ON WOUND HEALING IN ERBIL CITY/IRAQ

Mahabad Mohsin Abdullah[1], Payman Akram Hamasaeed[2], Khadija Khalil Barzani[3]

[1,2,3]Biology department, Education College, Salahaddin University - Erbil, Iraq, Mahabad.abdullah@su.edu.krd

Abstract

A problem facing modern medicine is wound infection caused by microorganisms that are resistant to drugs (MDR). To counter such a danger, new antibacterial agents like nanoparticles (NPs) are needed. The goal of this research is to identify a different treatment drug to fight the isolates of MDR Enterococcus hirae.

A total of 157 clinical specimens were obtained from various wounds and hospitals located in Erbil, Iraq, between July and October of 2022. 61 (38.21%) Gram positive bacteria (GPB) were found; based on 16S rRNA (PCR), sequencing, and the GenBank database, one (1.6%) of these was newly reported in Iraq. According to the findings of a sensitivity test conducted on 20 antimicrobials, E. hirae was resistant to 13 different antibiotics. Using an albino wistar rat model, zinc nanoparticles (ZnNPs) and silver nanoparticles (AgNPs) derived from Sesamum indicum seeds were biosynthesized and evaluated against isolated in vitro antibacterial and in vivo wound healing. In the current study, ZnNPs and AgNPs inhibition zones have 11 mm of antibacterial activity against E. hirae for each. With the standard therapies, the recovery period with ZnNPs and AgNPs creams was noticeably faster than that of usual therapy. Wounds infected with E. hirae that were treated with Zn NP, AgNPs, vaseline, fusidin, and mebo healed in 18, 16, 20, 24, and 21 days, respectively and the non-treated group healed in 39 days. The control (non-treated group) had slower healing times of wounds. The recent work is a significant step towards creating innovative nanoparticles that provide better alternative uses for antibacterial medications and wound treatments.

Keywords: Antimicrobial activity, Enterococcus hirae, Sesamum indicum seeds, AgNPs, ZnNPs, Wound healing.

1. Introduction

The issue of antimicrobial resistance is widespread. Antibiotic-resistant bacteria are thought to be the cause of an additional 23,000 fatalities annually in the United States and 25,000 deaths in the European Union. By 2050, this figure is predicted to increase to as many as 10 million deaths. Open wounds are the primary entry point for viruses into the body (1, 2). Numerous factors, such as cuts, burns, surgical operations, gunshot wounds, and underlying illnesses including diabetes and bedsores, can result in wounds and skin injuries. Hospital-acquired infections (HAIs) are serious concerns that require attention as public health hazards. Both society and healthcare organizations face serious challenges as a result of these illnesses. Antibiotic-resistant bacteria may spread fast, thus having germs in a wound can have devastating consequences and create significant medical and financial difficulties (3, 4). It is necessary to develop a new class of antimicrobials that are easy to use, safe, and usually effective. Additionally, an efficient strategy to prevent antibiotic resistance is to use a multidisciplinary treatment approach (5).

Nanotechnology has led to the development of particles ranging in size from 1 to 100 nanometers. This has led to innovative medical approaches for wound healing and the potential for new therapeutic strategies to combat diseases. The most researched, commonly utilized, and commercialized nanoparticles for numerous biomedical applications are ZnNPs, with a special emphasis on their usefulness in wound care (5, 6).

ZnO-NPs have also been shown to be safe for consumption by the US FDA, and their remarkable wound-healing, catalytic, bio-imaging, antibacterial, and anti-inflammatory properties make them highly suggestive for use in biomedical therapies. Due to its therapeutic synergy, ZnO-NPs are being explored as a potential drug delivery system for traditional medications (7). Moreover, NPs have a critical role in skin function by encouraging the creation of collagen, which speeds up the healing process of wounds. Furthermore, zinc is important for the skin epithelialization process of medications (8).

From decades, silver and zinc salts have been used to prevent the growth of different microbes from human. They have been widely studied for their antimicrobial efficacy against a range of bacterial strains. For instance, AgNPs have gained as antimicrobial coating for devices and ZnNPs have shown promising antimicrobial effects and has gained a focus in research and industries. ZnNPs and AgNPshave been extensively studied for their activity against pathogenic bacteria like *S. aureus* (9-12).

The use of plants in traditional medicine continues to be important around the world. According to the World Health Organization (WHO), a large population (80%) employs herbal remedies based on medicinal and aromatic plants to provide primary health care (13).

Sesamum indicum seeds has been reported by a variety of in vitro and in vivo studies as well as clinical trials have shown the therapeutic potential, which is known to contain a variety of bioactive compounds, including phenolic compounds, amino acids, fatty acids, and lignans, They have also been shown to possess a wide range of biological activities such as antioxidant, anticancer, antimicrobial, anti-inflammatory, blood lipid regulation, cholesterol reduction, liver and kidney protection, cardioprotective activity and other effects, that are beneficial to human health. It is widely grown and has a mellow flavor and high nutritional value, making it very common in the diet (13, 14). Using metal nanoparticles and their oxides is a potential strategy to break the resistance of bacteria to antibiotics.

In order to evaluate the antibacterial effectiveness of synthesized *S. indicum* seeds nanoparticles (ZnNPs and AgNPs) against the multidrug-resistant newly identified GPB, *E. hirae*, in vitro and in vivo as well as wound healing were the main objectives of this work.

2. Materials and Methods

2.1. Isolation and Identification of GPB

Between July and October 2022, 157 clinical samples, including those from gunshot wounds, burns, surgeries, diabetic ulcers, and bedsores, were collected from multiple hospitals in the Erbil, Iraq area. Every specimen was immediately put into blood agar that was selective for GPB, and then incubated for 24 hours at 37 °C. GPB were identified using colonial morphology, Gram stain, and molecular identification by the PCR (16S rRNA) gene. The primers used were 27F (AGAGTTTGATCCTGGCTCAG) and 1492R (TACGGYTACCTTGTTACGACTT), followed by sequence (15, 16). A web-based interface was employed to make the submission procedure easier (https://submit.ncbi.nlm.nih.gov). Every sequence has been submitted to GenBank, and all isolated bacteria are now assigned accession numbers.

2.2. Antimicrobial sensitivity test

The sensitivity of the isolated bacteria to 20 antimicrobials was evaluated using an antimicrobial sensitivity assay Amikacin (AK), Ampicillin(AMP), Amoxicillin-Clavulanic acid (AMC), Chloramphenicol (C), Ciprofloxacin (CIP), Cefotaxime (CTX), Doxycycline (DOX), Imipenem (IPM), Gentamicin (CN), Nalidixic acid (NA), Levofloxacin (LEV), Meropenem(MEM.), Nitrofurantoin (F), Norfloxacin (17), Rifampin (R), Streptomycin (S), Tobramycin(TOB.), Tetracycline (TE), Trimethoprim (TMP) and Vancomycin (VA) by using disc diffusion method (Kirby Bauer) as explained by Clinical and Laboratory Standards Institute (CLSI) (18).

2.3. Bio biosynthesis of ZnNPs and AgNPs using *S. indicum* seeds

2.3.1. Collection of *S. indicum* seeds

We obtained fresh *S. indicum* seeds from local markets in Shaqlawa, Erbil, and confirmed that they fit the category specified by Salahaddin University's College of Education in Erbil, Iraq.

2.3.2. Preparation of *S. indicum* seeds extract

After being cleaned with distilled water, sesame seeds were dried and ground. After mixing 20 g of seed powder with 100 ml of distilled water, the mixture was heated up for 45 minutes at 75 ºC. After being filtered twice using Whatman's filter paper, the extract from sesame seeds was kept at 4°C in preparation for more research. The filtrate served as a reducing agent during the production of nanoparticles (19).

2.3.3. Biosynthesis of ZnNPs and AgNPs

For zinc nanoparticles (ZnNPs) and silver nanoparticles (AgNPs) production, 100 ml of *Sesame seed* extract were added dropwise to 400 ml of 1 mM ZnO and 1 mM AgNO3 solutions under stirring separately. The resulting solutions were stirred for 2 hrs. at 1000 rpm and at 50ºC. The pH of solutions is controlled between 8-10 by adding Sodium hydroxide (NaoH). The solution was incubated for 72 hrs. at 37ºC. For the preparation of the powder of NPs, the solution was boiled on an electrical heater to evaporate the solvents, and the remaining powder was put in the oven for 2 hrs. at 200ºC for full sterilization and drying (19-21).

2.4. Characterization of ZnNPs and AgNPs

ZnNPs and AgNPs were screened in a scanning electron microscope (SEM) utilizing energy dispersive X-ray spectroscopy (EDX), Fourier Transmission Infrared Spectroscopy (FTIR), X-ray diffraction (XRD) measurements, and a double-beam UV-visible spectrophotometer to ascertain their chemical composition (22, 23).

2.5. Antibacterial activity of ZnNPs and AgNPs

ZnNPs and AgNPs were reported to have antibacterial action against MDR *E. hirae* in vitro using the well diffusion technique. Known concentration (0.1%) of 10 mg/ml (10,000 µl/ml) nanoparticles generated by dissolving 0.05 g of each nanoparticle in 5 ml ethanol and sonicating the solution for 1 hrs. at 50°C. The cultures were grown in BHI broth overnight at 37°C and then sub-cultured on MacConkey agar and incubated at 37°C for 24 hrs. A single colony from each plate was diluted in a sterile normal saline until the spectrophotometer read 0.08-0.13 turbidity at 630 nm to prepare a bacterial suspension at a final density of 0.5 McFarland standard $1.5x10^8$ CFU/ml. The suspension was spread on Mueller-Hinton agar and permitted to dry. Plates with wells of 7 mm diameter were filled with 150 µl of various NPs extract. The plates were incubated at 37°C for 24 hrs. After incubation, the zones of inhibition around the wells were measured (24, 25).

2.6. In vivo activity of Zn and AgNPs

2.6.1. Animal care and burn generation

For the experimental model, 200 ± 10 gm Wistar rats were used, which were female albinos. Two rats were housed in a 40 by 25 by 20 centimetre cage. The conventional care conditions, comprising a 12-hour photoperiod of light and dark, a temperature control set at 24 ± 2 °C, and continual access to food and drink, were consistently maintained. The experimental procedure was approved by the ethics committee and adhered to the ethical criteria for animal experimentation set out in Directive 2010/63/EU (26, 27). Before the experiment began, the rats were given a seven-day lab adaptation period. Initially, an intramuscular injection of 2% xylazine and 10% ketamine (10+90 mg/kg body weight) was administered to induce anesthesia in 12 rats (n = 2). After that, expert clippers were used to remove the hair. To create burn wounds of a specific thickness, a solid stainless-steel bar (Figure 1A) was heated for five seconds on predefined 4 cm2 sections of the animal's dorsal proximal region (Figure 1B) (28, 29). To demonstrate the inhibitory effects of the synthesized ZnNPs on antibacterial and wound healing activities, pure cultures of activated *E. hirae* were inoculated into the burned rats. The activated culture

(Figure 1C) and therapy (Figure 1D) were applied to each burnt rat's wound, and the cultures were allowed to proliferate for one entire day (29, 30).

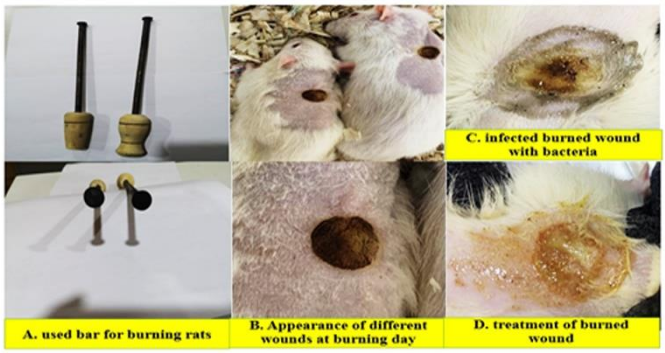

Figure 1: Burn generation

2.6.2. Preparation of Creams and wound treatment

ZnNPs and AgNPs creams were made by dissolving 0.05 gm of ZnNPs in 2 ml of dimethyl sulfoxide (DMSO) in a crucible to produce a concentration of 1% w/w. After adding 5 gm of pure vaseline wax, the mixture was heated for an hour at a moderate 500 rpm on a magnetic stirrer hot plate to dissolve the vaseline and combine it with each NPs separately. To make a homogeneous cream, the mixture was also chilled to room temperature while being stirred. Lastly, the mixture was sterilized for a further 15 minutes at 121°C (15 Ib/in2) in an autoclave using steam heat. The sterilized cream was then continuously churned and refrigerated (Figure 2) (8, 29). The burnt rats were divided into four major groups at random: the standard group (n = 2) got mebo 0.25% and Fusidin 2%); pure Vaseline wax served as the positive control; the test group received ZnNPs cream; and the negative control received no treatment. The wound was treated by swabbing it with the ZnNPs cream once per 24 hours after the infection had persisted for 24 hours (Figure 1D) (29, 31). Daily healing times were noted until the wound was completely closed.

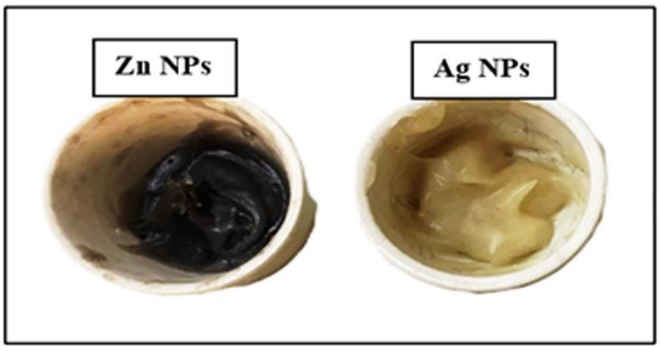

Figure 2: Prepared nanoparticle creams

2.7. Oral acute toxicity

2.7.1. Single dose toxicity study

Acute oral toxicity testing was performed on female wistar albino rats weighing 200 ± 10 gm to evaluate the toxicity of each nanoparticle in a living system. The test used an up-and-down pattern as defined in OECD exam Guidelines 425 (OECD, 2008). The rats had an overnight fast and a week of adaptation prior to the dosing (32).

2.7.2. Dose preparation and administration

The required amount of the compounds under investigation (mg/kg) in proportion to body weight was dissolved using ethanol. Then, as indicated in table (1), corn oil was added as a carrier, and the mixture was heated gradually while being agitated to achieve homogeneity and ethanol evaporation (29). Each of the four rats was administered an oral dosage of the limited test dose (2000 mg/kg) based on body weight, either twice via stomach tube gavage or once over the course of a 24-hour period. The rats were weighed according to with (OECD 425-27). Each animal was watched every day for the next 14 days following the dose administration, and then on an intermittent basis for the first 24 hours. Throughout the investigation, each rat had further observations to compare its condition to that of the control group. These observations included modifications to the eyes, skin, and hair in addition to behavioral changes (33). On day 15, the rats were euthanized, put to death with a mixture of xylazine 2% and ketamine 10%, and their external surfaces and abdominal organs were examined under a microscope (33, 34).

Table 1: Dose preparation and administration

Conc. mg/kg	Ethanol (mL)	Vehicle (mL)	No. of doses in 24 hours	No. of used rat	Lethality
2000	2	3	1	1	No
3000	2	3	1	1	No
4000	4	5	2	2	No
5000	4	5	2	2	No

3. Results

According to molecular research (PCR) using 16S rRNA, sequencing, and submission to the NCBI, the separate species *E. hirae* was found for the first time in Iraq in this study. The accession number for this strain is OQ378919.

3.1. Antimicrobial susceptibility

E. hirae was completely resistant to 13 of the 20 antimicrobials tested, including amikacin, chloramphenicol, ciprofloxacin, tobramycin, doxycycline, imipenem, levofloxacin, nalidixic acid, norfloxacin, rifampin, streptomycin, tetracycline and trimethoprim. However, it was responsive to the remaining antibiotics.

3.2. Biosynthesis of ZnNPs and AgNPs

The first sign of ZnNPs and AgNPs from *S. indicum* seeds was the colour change after 24 hours of mixing 100 ml *S. indicum* seeds extract with 400 ml of 1mM ZnO and $AgNO_3$ solutions, separately. ZnO and *S. indicum* seeds changed colour from light yellow to yellowish brown (tan or caramel colour); $AgNO_3$ and *S. indicum* seeds changed colour from light yellow to brown. Figure (3) shows that the change in colour of the solutions was seen visually ZnNP and AgNPs production were confirmed.

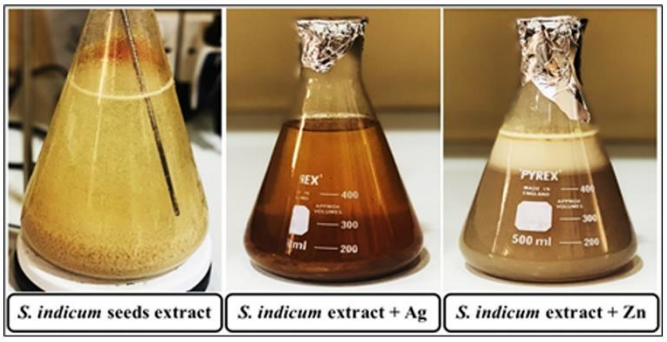

Figure 3: Inspection visually of the colour shift of nanoparticles

3.3. Characterization of ZnNPs and AgNPs from *S. indicum* seeds

3.3.1. UV-Visible Spectroscopy

A UV-Visible spectrophotometer was used to study NP synthesis. ZnNPs at 345 nm, ZnNPs (Figure 4A) displayed a noticeable plasmon absorbance band and AgNPs at 421 nm recording absorbance from 200-800 nm, prominent plasmon absorbance band was found (Figure 5A).

3.3.2. Fourier Transmission Infrared Spectroscopy

Several absorption bands were visible in the FTIR spectrum for ZnNPs and AgNPs generation from the extracts of sesame seeds in this investigation (Figure 4B and 5B). From ZnNPs a total of 1141.86, 1377.17, 1446.61, 1562.34, 1624.06, 1745.58, 2852.72, 2924.09, 3007.02, and 3394.72 cm−1 were the observed peaks. Bands of 723.31, 781.17, and 966.34 indicated C=C bending of the alkene, while the absorption band at 619.15 demonstrated the presence of C-Br stretching of the halo complex. The presence of C-H bending (aldehyde) and C-N stretching (secondary amine) was also verified by peaks at 1141.86 and 1377.17, respectively. Peak 1446.61 shows that an alkene has C-H bending. Peak observations of imines with C=N stretching was made at 1624.06, and peak observations of esters with C=O stretching were made at 1745.58. The peak at 1562.34 verified that the nitro compound's N-O functional group was present. Alkene was seen at the peaks of 2852.72, 2924.09, and 3007.02 with C-H stretching. N-H stretching at peak 3394.72 confirmed the presence of an alpha-amino acid. These vibrations all demonstrated the involvement of different biomolecules in the stability and reduction of NPs (19). While, AgNPs FTIR investigations revealed the spectra of silver nanoparticles between 400 and 4000 cm-1, with an absorption band around peak 723.31 indicating the existence of C=C bending of the alkene compounds. Secondary and tertiary alcohol with C-O stretching was identified at peaks of 1099.43 and 1163.08, respectively. The peak at 1240.23 confirms the presence of amines' C-N stretching functional groups. Peaks at 1382.96 and 1465.90 indicated the presence of the C-H bending functional group of aldehyde and alkene. At 1541.12, a nitro molecule with N-O stretching was detected. Imine/oxime has been established by a peak at 1647.21 with C=N stretching. Peaks at 1745.58 and 3339.76 indicated the presence of C=O stretching (esters) and N-H stretching (secondary amine). C-H stretching at peaks 2854.65, 2926.01, and 3007.02 revealed the presence of an alkene molecule. Also, this outcome agree with findings were found by Bekmezci, Ozturk (35).

3.3.3. X-ray differentiation (XRD)

The green produced ZnNPs' XRD diffraction spectrum showed peaks at 2θ (31.668 and 34.372) that matched the Zn (100) and (002) planes of the standard XRD (Figure 4C). According to the XRD design, ZnNPs are naturally crystalline. Zinc was found in two planes, one stronger than the other, at position 101 in the XRD pattern. ZnNPs were found to have an average size of 9.07 nm (19). The AgNPs structure revealed by XRD clearly demonstrated that the AgNPs were generated by the bio reduction of Ag ions by sesame seeds. The XRD spectrum revealed three strong peaks (38.227), (44.559) and (64.710) corresponding to the (011), (020), and (022) planes, respectively (Figure 5C). X-ray differentiation investigation revealed that the AgNPs were pure Ag monocrystal structures.

3.3.4. EDX spectroscopy

Furthermore, Zn and Ag presence are confirmed by clearly defined peaks in the elemental analysis obtained using EDX. In the EDX spectroscopy of ZnNPs, the maximum intensity zinc absorption peak at 2 keV was seen (Figure 4D), indicating that surface plasmon resonance led to the development of metallic ZnNPs that were crystalline in nature. In addition, The EDX spectroscopy of AgNPs revealed the maximum intensity absorption peak of silver at 2 keV (Figure 5D), demonstrating the development of metallic AgNPs that are crystalline in nature owing to surface plasmon resonance.

3.3.5. Scanning electron microscopy (SEM)

ZnNPs and AgNPs was examined using SEM. ZnNPs produced by treating zinc oxide solution with *S. indicum* seed extract. SEM showed that NPs had a spherical shape with an average size of 70 nm. The ratio of zinc sulphate to seed extract and the extract concentration determine the size and shape of the nanoparticles (NPs) (Figures 4E). AgNPs regularly formed, spherical shape was confirmed the existence of AgNPs by SEM images (Figures 5E).

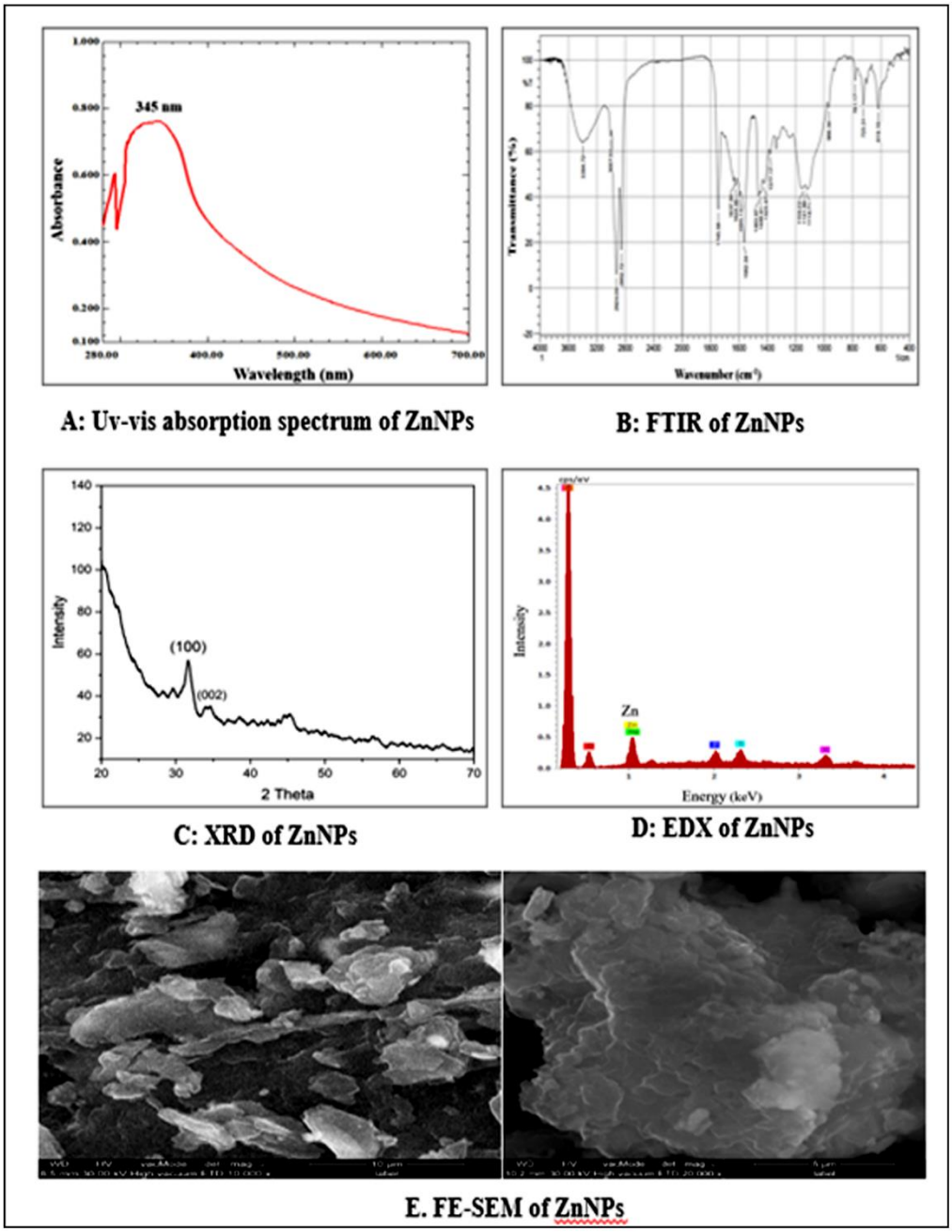

Figure 4: Characterization of ZnNPs

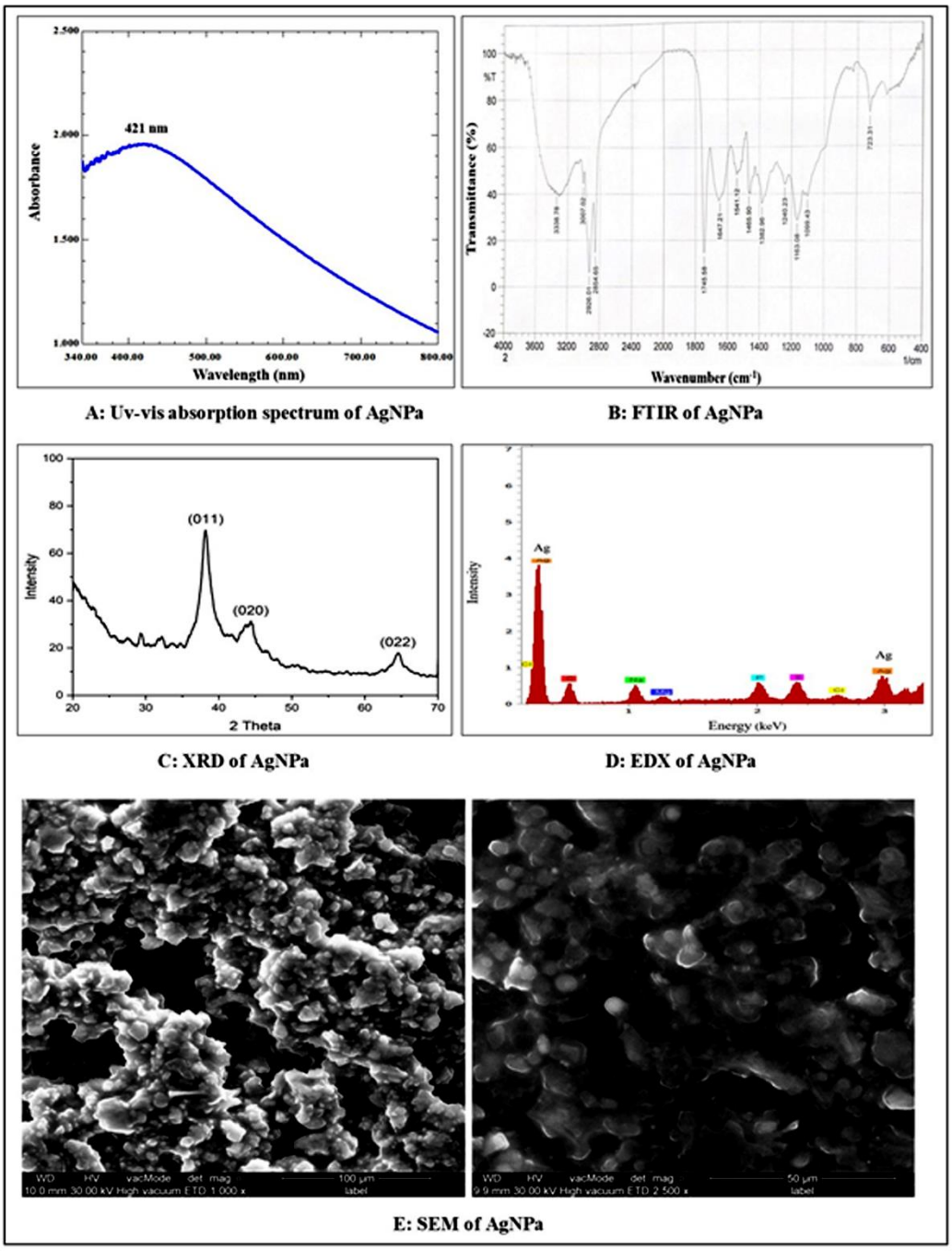

Figure 5: Characterization of AgNPs

3.4. In vitro antimicrobial activity of ZnNPs and AgNPs

ZnNPs and AgNPs with a 0.1% concentration were tested for their antibacterial action against *E. hirae*, and the results showed a 11 mm inhibitory zone for each nanoparticle. As demonstrated by these results have antibacterial properties as in table (2).

Table 2: Inhibition diameters of ZnNPs and AgNPs against isolated under the study

Nanoparticles	Zone of inhibition (mm)
	E. hirae
ZnNPs	**11**
AgNPs	**11**

3.5. In vivo antimicrobial and healing activity of ZnNPs and AgNPs

Until the wound was fully closed, daily records of the healing process were kept. As shown in as in table (3) and figure (6), wounds treated with nanoparticle creams of ZnNPs and AgNPs markedly demonstrated faster healing times compared to standard therapies.

Table 3: Healing time of treated rat wounds under the study

Nanoparticles	Healing time (days)
	E. hirae
ZnNPs	18
AgNPs	16

Vaseline (Positive Control)	20
Fusidin (Standard Control)	24
Mebo (Standard Control)	21
Non-treated (Negative Control)	39

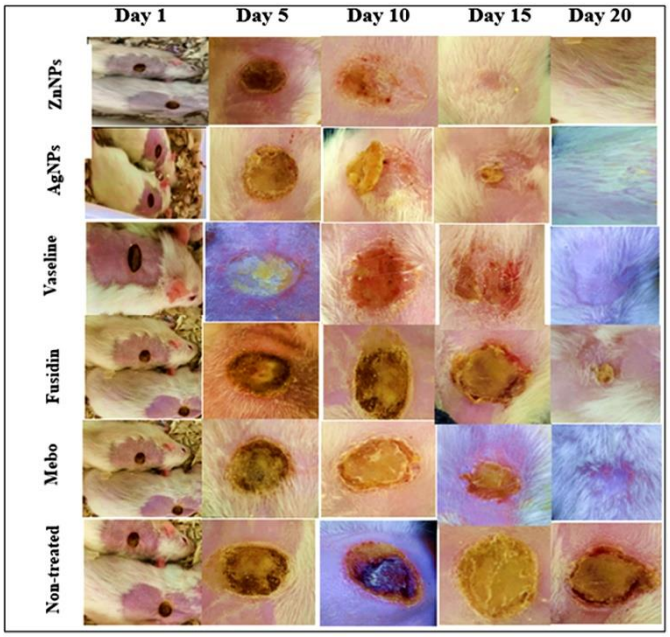

Figure 6: Wound healing on different days with ZnNPs, AgNPs, positive control, standard control and negative control

3.6. In vivo toxicological study (Acute oral toxicity)

Throughout the testing, the rats exhibited no overt poisoning symptoms, and no deaths were noted. These results suggest that the investigated nanoparticles could not be dangerous. At the conclusion of the research, the rats were administered anesthetic before being put to death. Macroscopical testing was performed on the abdominal organs to evaluate any potential changes associated with toxicological outcomes. Notably, no appreciable differences were observed between the test and control groups, indicating that the administration of ZnNPs and AgNPs does not appear to cause any toxicological problems. This comprehensive evaluation supports the safety profile of ZnNPs and AgNPs and raises the possibility that they will be employed in additional biological applications.

4. Discussion

Treating injuries and infections caused by MDR bacteria is an extremely difficult task. Because of this, concentrating efforts to address this problem is essential to delivering improved health care. This study aimed to investigate MDR in wound isolates obtained from patients who visited several hospitals in Erbil city-Iraq. Out of 157 wound specimens collected during this study, and, depending on molecular study (PCR) using 16S rRNA gene sequence analysis, 60 (38.21%) GPB identified in different wounds. (Khan et al., 2008, Kaftandzieva et al., 2012, Wan et al., 2021) findings aligned with ours concerning the percentage of GPB, as 36.25%, 42.11% and 30% respectively of all isolates were GPB present in wound infections.

The identification of a new kind of GPB (*E. hirae*) in Iraq in burn wounds. *E. hirae* understanding the features of these bacteria in the conditions of burn wounds is critical for developing successful treatment techniques and improving overall understanding of wound infections. *E. hirae* is a species of Enterococcus and small gram-positive cocci, catalase-negative, non-spore-forming bacteria, gray and non-hemolytic. Since then, it has been often found in different animals, but extremely rare cases were described in humans, also cause endocarditis and sepsis in humans (36).

On the other hand, the results of ZnNPs and AgNPs revealed that they had a potential effect on MDR bacteria and could inhibit bacterial growth. Various suggested mechanisms show that nanoparticles can alter bacterial survival rates. When NPs attach to bacterial cell membranes, they affect essential activities such as respiration and permeability. As a result, these nanoparticles enter bacterial cells, causing pits to develop in the membranes. Furthermore, zinc and silver metal or ions cause the formation of free radicals and reactive oxygen species (37), which may damage DNA and denature proteins, eventually leading to bacterial death (38).

Wound treatment in medical care is difficult because of their increased susceptibility to bacterial infections. Furthermore, there is a critical requirement for quick and efficient wound healing that reduces unwanted scarring. This work shows the potential of specific ZnNPs and AgNPs in therapeutic creams to improve wound healing, which is delayed by MDR *E. hirae* infection. The findings provide light on the potential of nanoparticle-based lotions in promoting wound healing in complicated infections. ZnNPs and AgNPs showed encouraging outcomes, with shorter healing durations compared to standard therapies and controls. Similar findings reported by El-Banna, Youssef (39), the study showed that wound healing was significantly faster in the groups treated with nanoparticles compared to other groups, conversely, the control non-treated group had slower healing times of wounds. AgNPs stand out as highly efficient in wound healing after 16 days. Their distinctive properties indicate that they can not only prevent wound infections effectively but also accelerate the wound healing process compared to conventional topical treatments (40). In addition, the alignment between the current findings and the study conducted by Pino, Bosco (41) provides valuable support for the observed wound healing properties of the ZnNPs. Pino, Bosco (41) who focusing on wound healing utilizing an animal model (albino wistar rats) found that ZnNPs resulted in fast healing after 17 days. This discovery is similar with the results of the current investigation, which indicated a healing duration of ZnNPs 18 days, indicating a consistent and powerful wound healing effect linked with the use of ZnNPs.

Nanoparticles may have antibacterial and regenerative capabilities that speed up the healing process and can eliminate bacteria and promote skin renewal (42).

Furthermore, the skin directly exposed to ZnNPs and AgNPs exhibited no observable changes or alterations in the appearance and structural composition. Hence, the tested concentration of ZnNPs and AgNPs is considered safe for application in topical medical treatments as an alternative antimicrobial therapy, the same results revealed by Escárcega-González, Garza-Cervantes (37) and Abdelsattar, Kamel (43). Currently, the science of pharmacology and toxicology need increased non-toxic therapeutic options that are more effective and have superior antibacterial activity against infectious illnesses caused by

diverse bacterial strains, notably MDR in clinical settings. As a result, the biosynthesis of ZnNPs and AgNPs, followed by cream creation, is acknowledged as a highly successful, cost-efficient, and simple way for developing a topical therapeutic with increased wound healing capabilities. These findings provide important insights for the development of innovative wound healing medications. To elucidate the mechanism of this influence, more detailed experimental data will be necessary.

5. Conclusion

The current work reports on the production of Zn and Ag nanoparticles from *S. indicum* seeds. The study looked at their in vitro antibacterial capabilities and in vivo excision wound healing activities in wistar rat models, with a focus on nanoparticle cream formulations. Zn and Ag nanoparticles were characterized via vital instrumental analysis. The findings showed that ZnNPs and AgNPs significantly inhibited the development of MDR *E. hirae*. This work demonstrated ZnNPs' and AgNPs effects as a non-toxic, cost-efficient, and promising choice for topical treatments in successful wound healing. Furthermore, ZnNPs and AgNPs revealed the potential to repair excision wounds in just 18 and 16 days respectively. Additionally, the current work poses a significant challenge in the development of innovative ZnNPs and AgNPs for antibacterial medications and wound creams, resulting in enhanced alternative uses. It provides to a better knowledge of the biological effects caused by important ions, opening the path for a new paradigm in medical research.

References

1. Lim C, Takahashi E, Hongsuwan M, Wuthiekanun V, Thamlikitkul V, Hinjoy S, et al. Epidemiology and burden of multidrug-resistant bacterial infection in a developing country. elife. 2016;5:e18082.

2. Al-Naqshbandi AA, Hassan HA, Chawsheen MA, Qader HHA. Categorization of bacterial pathogens present in infected wounds and their antibiotic resistance profile recovered from patients attending rizgary hospital-erbil. ARO-THE SCIENTIFIC JOURNAL OF KOYA UNIVERSITY. 2021;9(2):64-70.

3. Alavi M, Nokhodchi A. Antimicrobial and wound healing activities of electrospun nanofibers based on functionalized carbohydrates and proteins. Cellulose. 2022;29(3):1331-47.

4. Raoofi S, Pashazadeh Kan F, Rafiei S, Hosseinipalangi Z, Noorani Mejareh Z, Khani S, et al. Global prevalence of nosocomial infection: A systematic review and meta-analysis. PloS one. 2023;18(1):e0274248.

5. Hemmati J, Azizi M, Asghari B, Arabestani MR. Multidrug-Resistant Pathogens in Burn Wound, Prevention, Diagnosis, and Therapeutic Approaches (Conventional Antimicrobials and Nanoparticles). Canadian Journal of Infectious Diseases and Medical Microbiology. 2023;2023.

6. Nqakala ZB, Sibuyi NR, Fadaka AO, Meyer M, Onani MO, Madiehe AM. Advances in nanotechnology towards development of silver nanoparticle-based wound-healing agents. International Journal of Molecular Sciences. 2021;22(20):11272.

7. Abduljabbar B, El-Zayat M, El-Amier Y, El-Halawany E-S. Biosynthesis, characterization, and cytotoxic activities of zinc nanoparticles (ZnNPs) using Euphorbia retusa extract. Kuwait Journal of Science. 2023:100108.

8. Kantipudi S, Sunkara JR, Rallabhandi M, Thonangi CV, Cholla RD, Kollu P, et al. Enhanced wound healing activity of Ag–ZnO composite NPs in Wistar Albino rats. IET nanobiotechnology. 2018;12(4):473-8.

9. Irfan M, Munir H, Ismail H. Moringa oleifera gum based silver and zinc oxide nanoparticles: green synthesis, characterization and their antibacterial potential against MRSA. Biomaterials research. 2021;25(1):17.

10. Kareem M, Bello I, Shittu H, Sivaprakash P, Adedokun O, Arumugam S. Synthesis, characterization, and photocatalytic application of silver doped zinc oxide nanoparticles. Cleaner Materials. 2022;3:100041.

11. Alzubaidi AK, Al-Kaabi WJ, Ali AA, Albukhaty S, Al-Karagoly H, Sulaiman GM, et al. Green synthesis and characterization of silver nanoparticles using flaxseed extract and evaluation of their antibacterial and antioxidant activities. Applied Sciences. 2023;13(4):2182.

12. Raja FN, Worthington T, Martin RA. The antimicrobial efficacy of copper, cobalt, zinc and silver nanoparticles: alone and in combination. Biomedical Materials. 2023;18(4):045003.

13. El Hanafi L, Mssillou I, Nekhla H, Bessi A, Bakour M, Laaroussi H, et al. Effects of Dehulling and Roasting on the Phytochemical Composition and Biological Activities of Sesamum indicum L. Seeds. Journal of Chemistry. 2023;2023.

14. Wei P, Zhao F, Wang Z, Wang Q, Chai X, Hou G, et al. Sesame (Sesamum indicum L.): A comprehensive review of nutritional value, phytochemical composition, health benefits, development of food, and industrial applications. Nutrients. 2022;14(19):4079.

15. Dos Santos HRM, Argolo CS, Argôlo-Filho RC, Loguercio LL. A 16S rDNA PCR-based theoretical to actual delta approach on culturable mock communities revealed severe losses of diversity information. BMC microbiology. 2019;19(1):1-14.

16. Ugbo E, Anyamene C, Moses I, Iroha I, Babalola O, Ukpai E, et al. Prevalence of blaTEM, blaSHV, and blaCTX-M genes among extended spectrum beta-lactamase-producing Escherichia coli and Klebsiella pneumoniae of clinical origin. Gene Reports. 2020;21:100909.

17. Behera HS, Chayani N, Bal M, Khuntia HK, Pati S, Das S, et al. Identification of population of bacteria from culture negative surgical site infection patients using molecular tool. BMC surgery. 2021;21:1-7.

18. Rabie RA, Khattab F, Badr A, Alkady L. Association between methicillin susceptibility and biofilm production by Staphylococcus aureus colonizing atopic dermatitis patients and their impact on disease severity. Microbes and Infectious Diseases. 2023.

19. Zafar S, Ashraf A, Ijaz MU, Muzammil S, Siddique MH, Afzal S, et al. Eco-friendly synthesis of antibacterial zinc nanoparticles using Sesamum indicum L. extract. Journal of King Saud University-Science. 2020;32(1):1116-22.

20. Meva FEa, Segnou ML, Ebongue CO, Ntoumba AA, Kedi PBE, Deli V, et al. Spectroscopic synthetic optimizations monitoring of silver nanoparticles formation from Megaphrynium macrostachyum leaf extract. Revista Brasileira de Farmacognosia. 2016;26:640-6.

21. Fattahi A, Sakvand T, Hajialyani M, Shahbazi B, Shakiba M, Tajehmiri A, et al. Preparation and characterization of pistacia khinjuk gum nanoparticles using response surface method: evaluation of its anti-bacterial performance and cytotoxicity. Advanced Pharmaceutical Bulletin. 2017;7(1):159.

22. Ameen F, Altuner EE, Tiri RNE, Gulbagca F, Aygun A, Sen F, et al. Highly active iron (II) oxide-zinc oxide nanocomposite synthesized Thymus vulgaris plant as bioreduction catalyst: Characterization, hydrogen evolution and photocatalytic degradation. International Journal of Hydrogen Energy. 2023;48(55):21139-51.

23. Moghaddam FM, Jarahiyan A, Haris MH, Pazoki PY, Aghamiri B. High catalytic performance of CoCuFe2O4/ZIF-8 (Zn) nanocatalyst for synthesis of new benzimidazole derivatives. Journal of Molecular Structure. 2023;1285:135496.

24. Saravanan M, Vemu AK, Barik SK. Rapid biosynthesis of silver nanoparticles from Bacillus megaterium (NCIM 2326) and their antibacterial activity on multi drug resistant clinical pathogens. Colloids and Surfaces B: Biointerfaces. 2011;88(1):325-31.

25. Salem W, Leitner DR, Zingl FG, Schratter G, Prassl R, Goessler W, et al. Antibacterial activity of silver and zinc nanoparticles against Vibrio cholerae and enterotoxic Escherichia coli. International Journal of Medical Microbiology. 2015;305(1):85-95.

26. Zacharioudaki A, Kostomitsopoulos N. The contribution of veterinarians to the implementation of legislation on the protection of animals used for scientific purposes in Greece. Journal of the Hellenic Veterinary Medical Society. 2022;73(2):3913-20.

27. Marinou KA, Dontas IA. European Union Legislation for the Welfare of Animals Used for Scientific Purposes: Areas Identified for Further Discussion. Animals. 2023;13(14):2367.

28. Kim J, Dunham D, Supp D, Sen C, Powell H. Novel burn device for rapid, reproducible burn wound generation. Burns. 2016;42(2):384-91.

29. Samad MK, Hawaiz FE. Synthesis, characterization, antioxidant power and acute toxicity of some new azo-benzamide and azo-imidazolone derivatives with in vivo and in vitro antimicrobial evaluation. Bioorganic chemistry. 2019;85:431-44.

30. Zhu M, Liu P, Shi H, Tian Y, Ju X, Jiang S, et al. Balancing antimicrobial activity with biological safety: Bifunctional chitosan derivative for the repair of wounds with Gram-positive bacterial infections. Journal of Materials Chemistry B. 2018;6(23):3884-93.

31. Dwivedi D, Dwivedi M, Malviya S, Singh V. Evaluation of wound healing, anti-microbial and antioxidant potential of Pongamia pinnata in wistar rats. Journal of traditional and complementary medicine. 2017;7(1):79-85.

32. Olela B, Mbaria J, Wachira T, Moriasi G. Acute oral toxicity and anti-inflammatory and analgesic effects of aqueous and methanolic stem bark extracts of Piliostigma thonningii (Schumach.). Evidence-Based Complementary and Alternative Medicine. 2020;2020.

33. Zarei MH, Lorigooini Z, Khoei HA, Bijad E. Acute oral toxicity assessment of galbanic acid in albino rat according to OECD 425 TG. Toxicology Reports. 2023;11:111-5.

34. Wati H, Muthia R, Kartini K, Setiawan F. Acute toxicity study of the ethanolic extract of Eleutherine bulbosa Urb in Wistar rats. Pharmacy Education. 2021;21(2):143-7.

35. Bekmezci M, Ozturk H, Akin M, Bayat R, Sen F, Darabi R, et al. Bimetallic biogenic Pt-Ag nanoparticle and their application for electrochemical dopamine sensor. Biosensors. 2023;13(5):531.

36. Bollam R, Yassin M, Phan T. Detection of Enterococcus hirae in a case of acute osteomyelitis. Radiology Case Reports. 2021;16(9):2366-9.

37. Escárcega-González CE, Garza-Cervantes JA, Vazquez-Rodríguez A, Montelongo-Peralta LZ, Treviño-Gonzalez MT, Díaz Barriga Castro E, et al. In vivo antimicrobial activity of silver nanoparticles produced via a green chemistry synthesis using Acacia rigidula as a reducing and capping agent. International journal of nanomedicine. 2018:2349-63.

38. Hamad AH, Chawsheen MA, Al-Naqshbandi AA. Role of Laser Produced Silver Nanoparticles in Reversing Antibiotic Resistance in Some MultidrugResistant Pathogenic Bacteria. ARO-THE SCIENTIFIC JOURNAL OF KOYA UNIVERSITY. 2022;10(1):104-10.

39. El-Banna AH, Youssef FS, Youssef Elzorba H, Soliman AM, Mohamed GG, Ismail SH, et al. Evaluation of the wound healing effect of neomycin-silver nano-composite gel in rats. International Journal of Immunopathology and Pharmacology. 2022;36:03946320221113486.

40. Kithiyon M, Pannerselvam B, Balasaubramaniyam Madhukumar SS, Sridharan J, Alagumuthu TS. Efficacy of mycosynthesised AgNPs from Earliella scabrosa as an in vitro antibacterial and wound healing agent. IET nanobiotechnology. 2019;13(3):339-44.

41. Pino P, Bosco F, Mollea C, Onida B. Antimicrobial nano-zinc oxide biocomposites for wound healing applications: a review. Pharmaceutics. 2023;15(3):970.

42. Pormohammad A, Monych NK, Ghosh S, Turner DL, Turner RJ. Nanomaterials in wound healing and infection control. Antibiotics. 2021;10(5):473.

43. Abdelsattar AS, Kamel AG, Hussein AH, Azzam M, Makky S, Rezk N, et al. The Promising Antibacterial and Anticancer Activity of Green Synthesized Zinc Nanoparticles in Combination with Silver and Gold Nanoparticles. Journal of Inorganic and Organometallic Polymers and Materials. 2023:1-14.